Renewable and Sustainable Energy Reviews 181 (2023) 113339

Contents lists available at ScienceDirect

Renewable and Sustainable Energy Reviews

journal homepage: www.elsevier.com/locate/rser

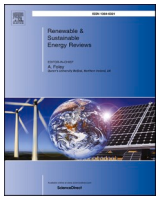

A critical analysis of the uncertainty in the production estimation of wind parks in complex terrains

Pier Francesco Melani [a], Federica Di Pietro [a], Maurizio Motta [b], Marco Giusti [c], Alessandro Bianchini [a,*]

[a] Department of Industrial Engineering, Università degli Studi di Firenze, Via di Santa Marta 3, 50139, Firenze, Italy
[b] EMD International, Niels Jernes vej, 10, 9220, Ålborg, Denmark
[c] AGSM AIM, Lungadige Galtarossa, 8, 37133, Verona, Italy

ARTICLE INFO

Keywords:
Annual Energy Production (AEP)
Complex terrain
Wind turbines
Uncertainty

ABSTRACT

Assessing the wind resource in complex terrains with the level of accuracy required by industry is not a trivial task. The present study critically analyzes the different elements involved in the process and how they affect the predicted Annual Energy Production (AEP) of a wind farm. Five different sites in Italy, for which the installing company had *a posteriori* AEP data available, are considered. All sites are modeled with the windPRO software. To separate the effects related to the quality of experimental measurements from those due to the selected wind modeling techniques, two different approaches were followed. In the "*horizontal*" one, the minimum amount of wind data common to all installation sites were used, i.e., the measurements of one mast at one selected altitude for a single full year, thus highlighting the role of the terrain modelling. In the "*vertical*" approach, the analysis focused on the site with the most complex terrain, using wind data of different quality and duration, as well as different processing techniques, from the ubiquitous WAsP to WAsP-CFD. The results of the study confirm that, even in presence of high-quality measurements and a standard workflow, the accuracy of the farm's AEP estimation is strongly site-dependent. For mildly-complex terrains, the lack of accuracy in mast data can be compensated with a more advanced spatial scaling method, and vice versa. On the other hand, in presence of steep slopes or sneaky ridges, attention must be paid to both the experimental and modelling components. A scaling approach based on Computational Fluid Dynamics (CFD) is mandatory. In all cases, thermal effects such as atmospheric stability must be carefully evaluated and included in the assessment process.

1. Introduction

Wind energy is expanding rapidly worldwide, with almost 850 GW of total installed capacity at the end of year 2021 [1]. Notwithstanding this, the Global Wind Energy Council (GWEC) [1] estimated that, at the current rate of installation, the available wind capacity by year 2030 will be one-third lower than that required to follow the 1.5 °C decarbonization pathway. Among the different factors contributing to this slowdown, one of the most relevant is the inherent difficulty in assessing the wind resource in non-standard terrains with the level of accuracy required by the industry. It should be remembered that, as the available power is proportional to the cube of the freestream wind speed, an error of less than 1 m/s in its estimation can correspond to millions of dollars of losses in annual revenues [2]. Recently, financial institutions have become aware of this issue, therefore raising the level of detail and reliability required to access funding [3].

Achieving this degree of accuracy is not an easy task using common state-of-the-art tools, especially when *complex terrains*, i.e., installation sites characterized by major orographic (mountains, valleys, ridges, etc.) and roughness (forests, lakes, etc.) features, are considered. These installations are anyhow receiving increasing attention from both industry and academia, not only due to the possibility of exploiting local speed-up and channeling phenomena to increase energy production, but also to the scarcity of "premium" onshore installation sites, i.e., sites with relatively flat terrain away from human settlements, especially in densely populated areas such as Europe [4].

A formal definition of "terrain complexity" as well as a quantitative index to evaluate it are not available yet. A first scoring system was proposed by Barber et al. [5], but their computation is mainly based on the opinion of the analysts and is therefore not completely objective. Nonetheless, the main features concurring to the definition of the wind

* Corresponding author.
E-mail address: alessandro.bianchini@unifi.it (A. Bianchini).

https://doi.org/10.1016/j.rser.2023.113339
Received 4 October 2022; Received in revised form 4 May 2023; Accepted 4 May 2023
Available online 6 May 2023

Nomenclature

Acronyms

ABL	Atmospheric Boundary Layer
AEP	Annual Energy Production
CFD	Computational Fluid Dynamics
MCP	Measure-Correlate-Predict
RANS	Reynolds-Averaged Navier Stokes
WAsP	Wind Atlas Analysis and Application Program
WI	Wind Index
WT	Wind Turbine

Greek symbols

α	Wake Decay Constant [−]

Latin symbols

CF	Sensitivity to uncertainty on wind speed [−]
C_P	Air specific heat coefficient [kJkg^{-1}K^{-1}]
C_T	Rotor thrust coefficient [−]
H_0	Ground average surface heat flux [Wm^{-2}]
I	Uncertainty on wind speed [ms^{-1}]
k	Von Kármán constant [−]
L	Monin-Obukhov length [m]
r	Wind speed correlation coefficient [−]
R	Rotor radius [m]
T_0	Ground surface temperature [K]
u^*	Friction velocity [ms^{-1}]
v	Wake wind speed [ms^{-1}]
V	Wind speed [ms^{-1}]
x	Streamwise coordinate [m]
Y	Number of concurrent years [−]
z	Altitude above ground level [m]
z_0	Effective roughness length [m]

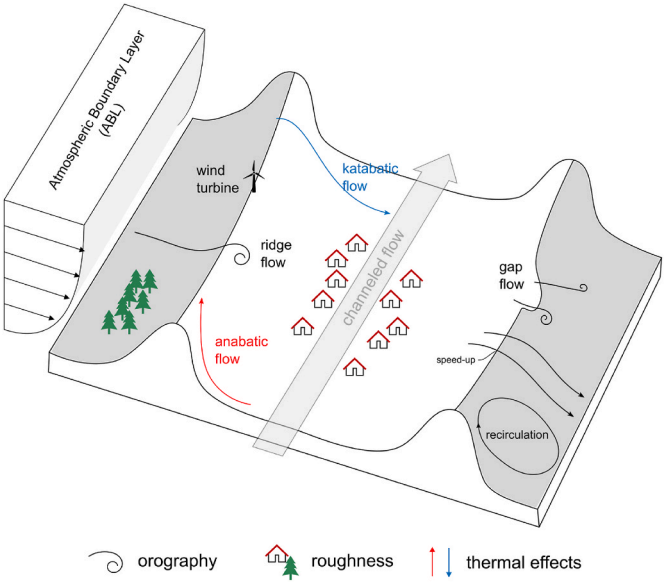

Fig. 1. Schematic representation of the local wind distribution in a mountain environment, adapted from Ref. [6].

field in a complex terrain can still be identified. These are illustrated in Fig. 1, taking as an example a typical mountain environment, and reported in Table 1, together with their effects on the Atmospheric Boundary Layer (ABL) and the modelling approaches currently available in the literature. The analysis is indeed *multi-disciplinary* [5], as the ABL is affected *mechanically* by the local topology, i.e., the combination of orographic and roughness features, and *thermally* by its interaction with the soil and the solar radiation. The latter can modify the stability of the atmosphere and induce time-varying secondary flows [6]. Since all these phenomena are strongly interconnected, the problem is also *non-linear* and therefore site-specific.

Early research on the topic made use mainly of experimental evidence, collecting wind data from on-field measurements and using them to synthesize the wind statistics for the site via dedicated methodologies. A comprehensive review of these approaches can be found in Lei et al. [22] and Murthy and Rahi [2]. Many examples of experimental investigations are available in the literature, some of them more oriented on the anemometric part, such as the famous campaigns of Fernando et al. on the Perdigão [6] and Materhorn [8] ridges, others on the evaluation of the local energy potential, as in the works of Chandel et al.

Table 1
Main features affecting the ABL on an installation site. Available modelling tools are also reported.

Name	Effects on the ABL	Modelling tools
Orography	- local speed-up and steering on ridges [6] and mountain passes [7] - possible separation on the leeward side of hills for slopes higher than 20–30% [8] - forced channeling in valleys [9]	- linear models (e.g., WAsP [10]) - Computational Fluid Dynamics (CFD) ([11–14]) - on-field measurements ([6,8,15])
Roughness	- deceleration of the ABL profile due to distributed roughness - displacement of the ABL profile due to concentrated roughness (e.g., cities, forests, canopies, etc …) [16]	- modification of the boundary layer law [17] - dedicated models for concentrated roughness (e.g. Ref. [18]) - Computational Fluid Dynamics (CFD) [19] - on-field measurements
Atmospheric stability	- seasonal and diurnal modification of the ABL stratification due to heat exchange with the ground [20]	- modification of the boundary layer law [20] - on-field measurements - Computational Fluid Dynamics (CFD) ([19,21])
Thermal cycling	- seasonal and diurnal acceleration/deceleration of the lower layers due to thermally-driven flows [15]	- on-field measurements ([6,8]) - Computational Fluid Dynamics (CFD)

in India [23] or Kucukali and Dinçkal in Turkey [24]. However, no standard procedure has been settled yet, making this aspect the largest source of uncertainty [3].

The main limitation of the experimental/statistic approach is that wind data are usually available in only few measuring spots. In sites such as the one represented in Fig. 1, however, the wind spatial distribution at the height of interest can vary significantly from the one predicted by data available at larger scales in both magnitude and direction [5]. A so-called *extrapolation model*, accounting for the physics of the different phenomena outlined in Tables 1 and is therefore required to extend the range of measured wind data from the mast location to turbine hubs.

To date, the approach followed by the scientific community has been to investigate each of these aspects individually. The most critical ones are *orography* and *roughness*, as their effects on the wind flow field are inherently three-dimensional and thus cannot be handled with lumped-parameters models [12]. Historically, linear approaches such as WAsP (Wind Atlas Analysis and Application Program) [10] (see Section 3.2 for details) have been extensively used in both academic and industrial applications [2], providing reliable results as long as the maximum slope

Table 2
Main characteristics of the installation sites under consideration.

Name	Year	Coordinates	Altitude [m]	# WTs	WT model	Hub height [m]	# Masts
Rivoli	2013	E 641′331 N 5′046′693	279.2	4 × 2 MW	Repower MM92	78.5	2
Affi	2017	E 639′963 N 5′046′734	239.4	2 × 2 MW	Senvion MM92	80	2
Casoni di Romagna	2008	E 693′787 N 4′902′448	741.2	16 × 0.8 MW	Enercon E53	60	2
Carpinaccio	2012	E 690′399 N 4′892′393	830	17 × 0.8 MW	Enercon E53	60	1
Riparbella	2012	E 631′169 N 4′806′461	540	10 × 2 MW	Vestas V90	80	1

did not exceed 20%–30% [12]. This limit has been verified in the works of Rathmann et al. [25] and Mortensen et al. [26] and has been overcome only recently with the advent of tools based on Computational Fluid Dynamics (CFD), such as WAsP-CFD [11] (see Section 3.3). Despite their higher complexity and computational cost, these approaches are able to deal with very complex terrains such as rocky islands [13] or steep mountain ranges [14]. On the other hand, thermal effects, and in particular *atmospheric stability,* have been included so far as semi-empirical correlations of the ABL law [20]. Due to the increasing necessity of more advanced modelling approaches, CFD investigations of these phenomena started to appear only in the last few years, with the simulation campaigns of Katraman et al. on Perdigão [19] and Letzgus et al. on the Bavarian Alps [21].

While individual aspects of the siting problem have been largely

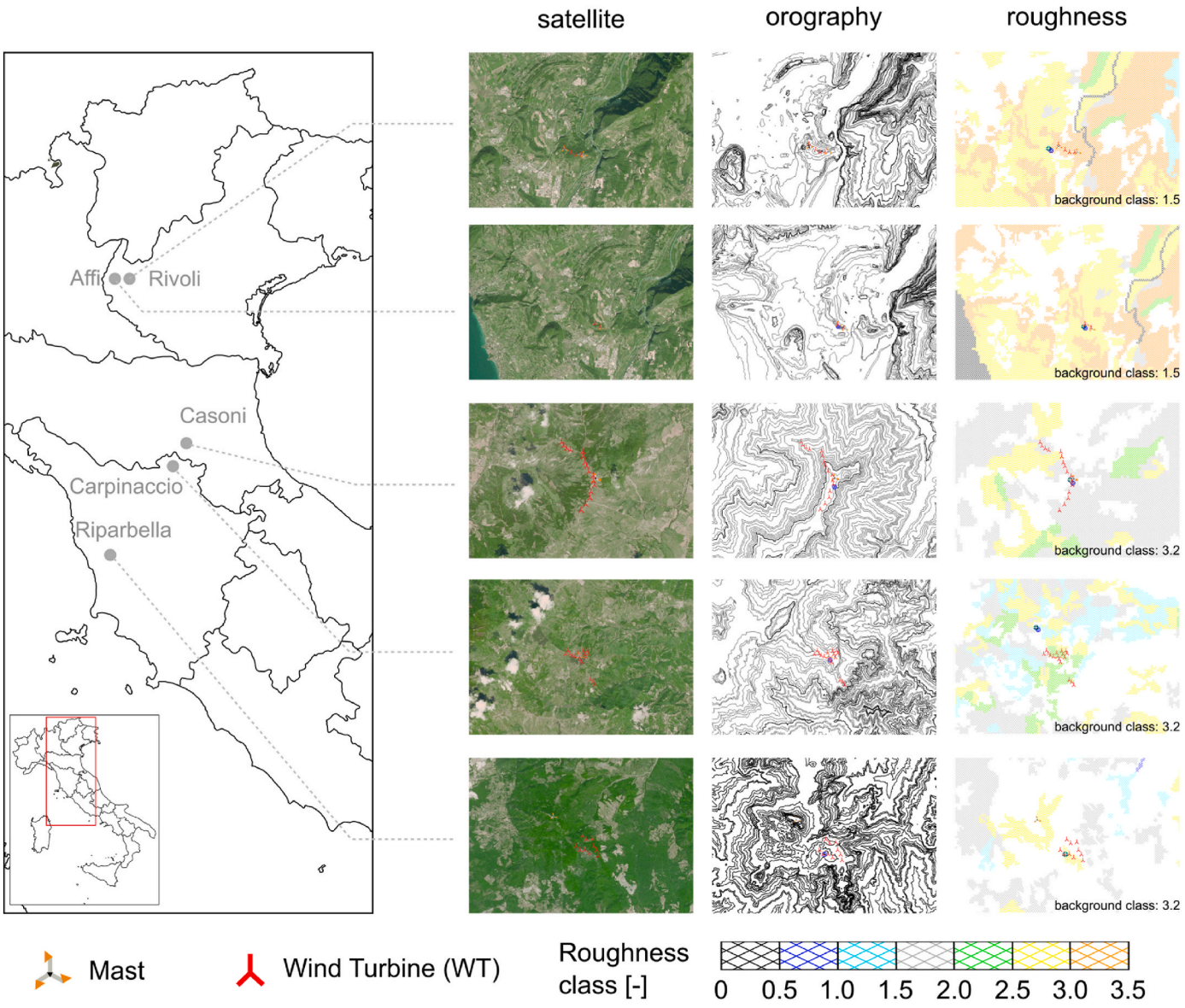

Fig. 2. Topological features of the installation sites under consideration.

covered by the cited studies, very few works are available in the literature that analyze how these elements combine together, and try to define their influence on the effective Annual Energy Production (AEP) of the wind farm. Progress in this direction was recently made by Barber et al. [27], who applied seven combinations of modelling tools to five different installation sites in complex terrains. The study highlighted how the performance of each workflow in predicting the measured wind data would change from one site to another due to the non-linear interaction between the local orography, the ABL, and solar radiation. It was also highlighted how the correlation between the prediction of the wind field and the AEP is not straightforward, indicating that additional effort is needed in that direction.

1.1. Outline of the study

This study investigates the impact of the different elements related to the assessment of the wind resource on the predicted AEP of a wind farm in complex terrain. Five sites in Italy are considered for the analysis, differing not only in terms of topology, with a level of complexity increasing from low hills to mountain valleys, but also in terms of accuracy and detail of on-site experimental wind data. The number of measuring points and altitudes, as well as the duration of the anemometric campaign, indeed varies from site to site.

The analysis was based on the standard workflow currently in use by industry for modelling wind parks. This makes use of the windPRO software in combination with the WAsP linear approach [10], which maps the wind resource based on the topological features (orography, roughness, obstacles, forests, etc.) of each installation site. For the most complex one under consideration, dedicated three-dimensional Reynolds-Averaged Navier-Stokes (RANS) simulations were performed via the WAsP-CFD tool [11].

In an attempt to separate the effects on the predicted AEP induced by the quality of experimental measurements from those related to extrapolation techniques, two different approaches were followed: a "*horizontal*" and a "*vertical*" one. In the horizontal one, the minimum amount of wind data common to all installation sites was used, i.e., measurements of one mast at one selected altitude for one year, thus highlighting the role of terrain modelling. In the vertical approach, the analysis focused on the site characterized by the most complex terrain, using wind data of different quality and duration as well as different preprocessing techniques. In this way, the sensitivity of the predicted AEP to the accuracy of the input wind data is assessed.

Eventually, production data obtained with the two approaches, along with the associated uncertainty, were validated against the historical ones provided by the company AGSM AIM SpA, which manages the considered wind farms. A relevant share of the value and novelty of the study indeed lies in these datasets, which, to the authors' knowledge, are for the first time available in such quantity and variety, at least for Italy.

2. Installation sites

Five operational wind farms in Italy, for which real AEP data were available from the installing company, were selected as test cases. An overview of their main characteristics, including the installed Wind Turbines (WTs), is reported in Table 2.

Selected sites do represent a valuable dataset for the scope of the analysis proposed herein, as they cover a variety of terrains of increasing complexity. This feature is particularly evident in Fig. 2. The site of *Riparbella* is in fact located in a mildly hilly area near the city of Pisa, while *Casoni di Romagna* and *Carpinaccio* are installed along the steep ridges of the Appennino Tosco-Emiliano mountain range, where they exploit a significant speed-up effect. Among considered locations, the most peculiar ones are *Affi* and *Rivoli*, which, as shown in Fig. 2, are positioned at the entrance of the narrow valley encompassing river Adige, next to Garda Lake, where the incoming wind is accelerated by the corresponding forced channeling effect [9]. *Rivoli*, in particular, is known to be a critical location, since it sits on a hill right next to the bed of the river. Therefore, it required higher-order methods for the mapping of the wind resource (WAsP-CFD) and was selected in the study as the test case for the *vertical* approach, i.e., the use of measured wind data of different quality and duration to assess their contribution to the accuracy of predicted AEP.

Table 3
Main characteristics of the wind measurement campaign for all sites under consideration.

Name	Mast ID	Acquisition heights [m]	Acquisition period [dd/mm/yyyy]	Availability [%]
Rivoli	1	20, 30, 40, 50	28/07/2006 - 31/05/2012	89.5
	2	30, 40, 50	13/12/2007 - 31/05/2012	90.9
Affi	1	40, 2 × 50	26/11/2008 - 30/11/2015	91.0
	2	40, 50, 2 × 65, 2 × 80	04/07/2014 - 30/11/2015	91.2
Casoni di Romagna	1	10, 30	06/12/2001 - 05/10/2006	72.9
	2	20, 2 × 30, 40, 50, 2 × 60	31/07/2005 - 05/10/2006	90.5
Carpinaccio	1	10, 20, 40	28/04/2004 - 22/03/2012	59.7
Riparbella	1	30	11/04/2003 - 17/01/2010	76.5

2.1. Site characterization – orography, roughness, and obstacles

For all considered installation sites, orography data were taken from the Italian Elevation Model - TINITALY [28] database, as it provides the maps with the highest spatial resolution (10 m) for Italian territory. To get sufficient coverage for WAsP calculations [10], elevation contours were imported for a square area of 24 km × 24 km around the center of the site.

The same strategy was adopted for terrain roughness data, for which a 50 km × 50 km squared area was considered. As a reference database, the European CORINE Land Cover 2018 [29] was selected, with a spatial resolution of 100 m. Imported data were then manually modified to accommodate the specific features of each installation site. For *Casoni*, *Carpinaccio* and *Riparbella*, the presence of extensive forests (see Fig. 2) implied the definition of a default, or background, roughness class of 3.2, estimated by crossing data from satellite images and the local forest management institute.

Finally, obstacles were manually identified from satellite maps and inserted into the site model as equivalent rectangular objects, as imposed by the WAsP approach, with a height and porosity dependent on the specific obstacle. This operation was performed only in proximity of the turbines and measurement masts, since obstacles in this area have the largest impact on the assessment of the wind resource.

2.2. Measured wind data

The starting point for the analysis was represented by experimental wind data collected on-site by the installing company AGSM-AIM SpA. All measurements were performed via a standard mast configuration, equipped with cup anemometers for wind speed, vanes for direction and thermometers for local temperature sampling. The number of masts and instruments, as well as the length of the measurement period, vary with the site under consideration, as reported in Table 3.

Fig. 3 compares the different measurement campaigns in terms of mast position, wind direction, and diurnal wind profiles at different altitudes. These latter were normalized over the average wind speed of the site V_{avg} at the highest available height, due to confidentiality issues. Installations in *Affi* and *Rivoli* present a basically mono-directional wind

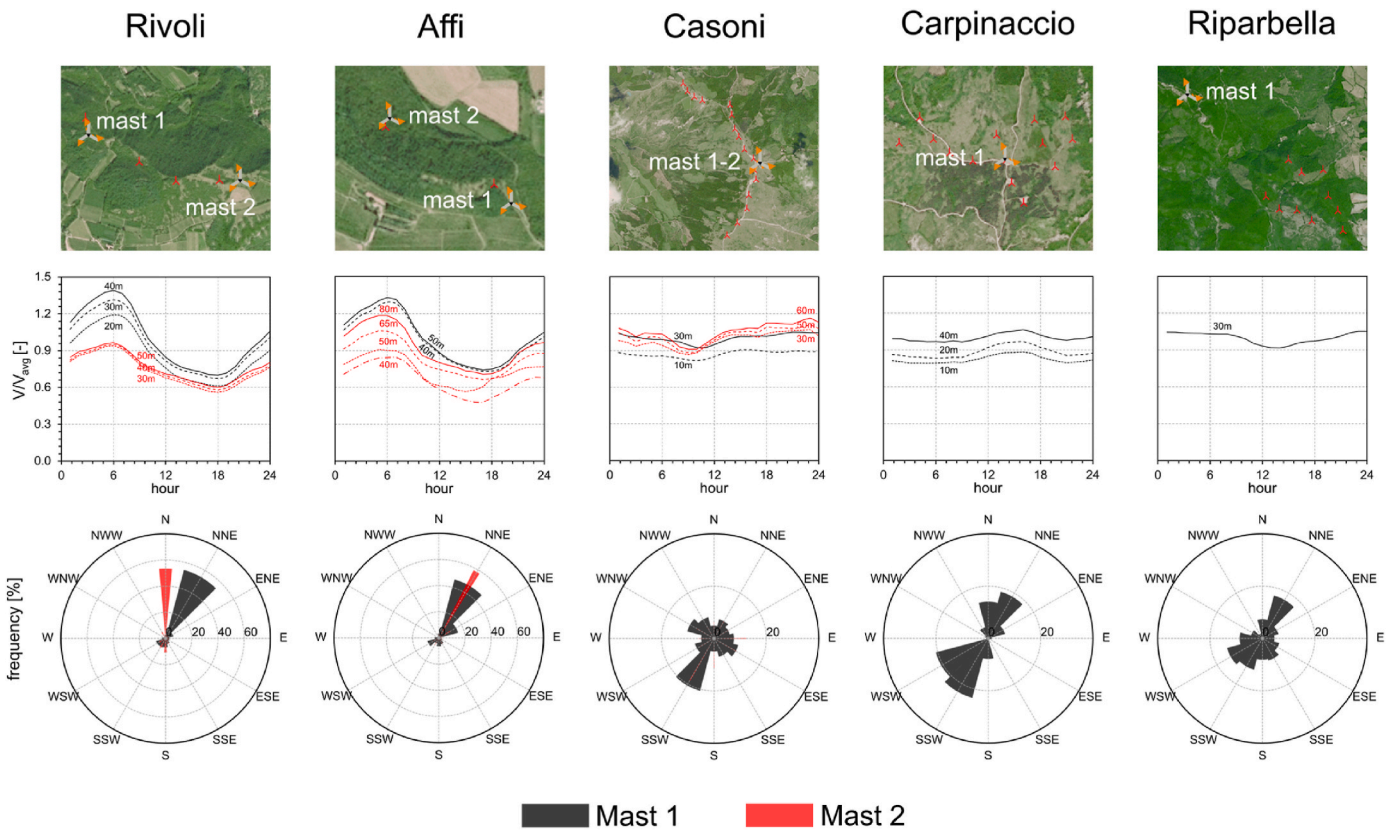

Fig. 3. Measured wind speed diurnal profile and direction for all sites under consideration.

profile, oriented at NNE towards the entrance of the Adige valley (see Fig. 2). The presence of the ridge notably distorts the wind distribution along its tip line, shifting progressively from an accelerated flow at *mast 1* to a steered (direction N) and slower one at *mast 2*. This effect is superimposed on a large diurnal variation of both wind intensity and vertical profile shape, likely due to thermal forcing effects coming from the valley nearby and the Garda Lake. When analyzing relatively simpler terrains such as *Casoni* and *Carpinaccio*, the influence of thermal forcing

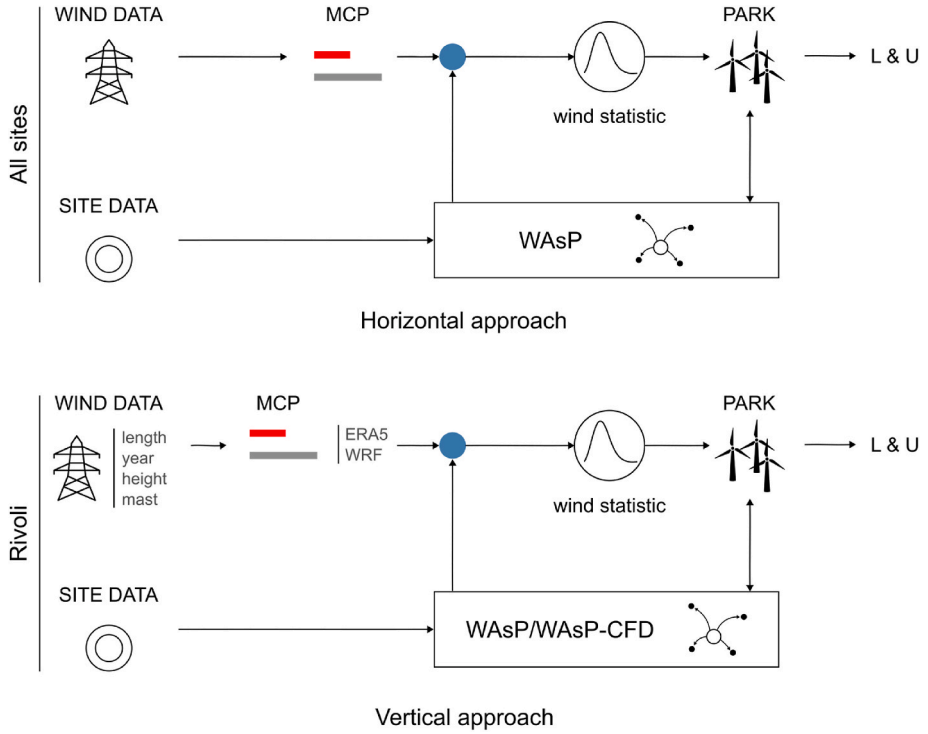

Fig. 4. Schematic comparison between horizontal and vertical analysis approaches.

fades away, leading to a fairly constant wind profile during the day. The lack of a second mast in these sites unfortunately does not allow to infer any characteristics of the spatial distribution of the flow along the ridges used for the installations, even though it seems to be aligned for most of the time with the less steep side of the mountain, along SSW-NNE direction. This allows exploiting the corresponding speed-up effect to increase power production. Finally, the site of *Riparbella* differs from all others, as the measuring mast is located on a different hill than the one where the wind farm is (since the park was acquired by the company at a later date). As it will be shown in Section 4.1, this notably increases the uncertainty related to the assessment of the wind resource.

Raw wind measurements were preliminary inspected to remove possible bias and measurement errors, so as to increase the overall quality of the input data for wind resource assessment. For example, temperature measurements were cross-compared with direction data from the vane to detect possible malfunctioning of the instrumentation due to icing.

3. Methodology

To decouple the influence on the predicted Annual Energy Production (AEP) of the methodology used for experimental wind data acquisition from that related to the modelling of site terrain, i.e., the extrapolation of mast measurements to turbine's hub height and location, two different approaches were adopted, defined as the "*horizontal*" and the "*vertical*" ones.

In the *horizontal approach*, input wind data of the same quality are used for all installation sites. More in detail, measurements from one mast at the highest altitude and with a minimum duration of one year were used. Only one reference database (EMD-WRF [30]), based on ERA5, was adopted to correct measured data for long-term effects ("Measure-Correlate-Predict", MCP [31]), as explained in detail in Section 3.1. To highlight the role of the uncertainty in modelling the terrain, the workflow schematically shown in Fig. 4 was then applied to each wind dataset. The WAsP linear extrapolation model [10] was first used to "filter out" the effects of terrain in the calculation of the general wind statistics for the site and then to map it back to the hub position of each wind turbine during the calculation of the AEP (PARK, see Section 3.4). The AEP, which represents the gross energy production of the farm, was eventually corrected for various losses and the uncertainties associated with the overall calculation (Losses & Uncertainties, L & U), according to the algorithm outlined in Section 3.5.

On the other hand, the *vertical approach* follows the same workflow, but it is applied only to the site with the most complex terrain, i.e., the wind farm of *Rivoli* (see Fig. 2). To highlight the influence of on-site wind measurements, different methodologies were adopted to select the wind data used as input to the flow model from raw experimental dataset. As reported in Fig. 4, several wind series, differing in terms of year and length of acquisition, reference altitude, and position of the mast were used for the analysis. On top of that, two different reference databases, namely ERA5 [32] and EMD-WRF [30], were selected for the MCP long-term correction. Given the configuration of the terrain under consideration, the classical WAsP linear approach was sided in this case with the more advanced, non-linear WAsP-CFD solver [11]. The corresponding set-up is described in Section 3.3.

3.1. MCP

Measured wind data might be biased by the inter-annual variability of the wind resource. To make sure that the year of measurement is not abnormal and thus represents the anemometric characteristics of the site in a statistically meaningful way, it is required to correct it based on a long-term wind dataset of at least 10–20 years from the same region [31]. This procedure is called MCP (Measure-Correlate-Predict) in windPRO and, as it will be shown in Section 4, plays a major role in determining the accuracy of the AEP estimation.

3.1.1. Reference wind dataset

A fundamental step in the MCP procedure is the selection of the 20-year reference dataset to be used for the long-term correction.

In this study, the ERA5 re-analysis database [32] was considered. Combining historical observations around the globe with an Earth climate model, this dataset covers the whole timespan from year 1950 to now with a temporal resolution of 1 h and a spatial resolution of 31 km, distributed over 137 height levels. Therefore, it represents one of the most complete references currently available. In virtue of the terrain complexity of the sites under consideration, corresponding to a large spatial variability of both wind speed and direction, reference data were needed at locations with flow conditions similar to those experienced by the measurement mast. To this end, ERA5 data were integrated with the EMD-WRF dataset [30]. The latter makes use of meso-scale simulations to refine the ERA5 spatial resolution down to 3 km.

Before undergoing the MCP correction, the quality of selected data series was rigorously checked to avoid the propagation of possible bias errors to later steps of the analysis. In addition to the evaluation of the similarity between the mast and reference series in the chosen concurrent period of one year, the presence of drifts (i.e., the increase or decrease of the annual average wind speed over the years) was highlighted via the Mann-Kendall (MK) test [33]. A threshold of 0.4 was established for the measured trend to be significant.

3.1.2. Correlation models

Once the quality of both 1-year short-term and 20-year long-term data has been verified, dedicated statistical methods were used to build a transfer function between the two for the year selected for the analysis (the concurrent period). This relationship was then used to generate the 1-year long-term corrected wind data series for use in the computation of the site general wind statistics, as outlined in Fig. 4.

Two different approaches have been adopted in the study. The first one is called *Local Scaling* and is based on a simple correction of the wind data measured by the mast V_{mast} in the form:

$$V_{mast,LP} = A * V_{mast} + B \quad (1)$$

where A and B depend on the ratio between the average wind speeds and standard deviations of the mast and reference series in the concurrent period. As this formulation preserves the local wind direction, it is usually recommended for situations in which local, high-quality data are available and the reference is deemed not able to reproduce these local directional conditions. This is the case of masts located in complex terrains with strong spatial gradients of both wind speed and direction. However, this method requires high-quality measurements as input, since possible aging or malfunctioning of the measuring vane cannot be corrected.

The second family of correlation methods adopted herein is based on the generation of the long-term corrected wind data from the reference dataset. As this also implies the modification of the local wind direction, these formulations are usually recommended when a good correlation between short- and long-term data is available.

Four different options are available in windPRO:

a. *Linear regression:* a linear relationship is used to build the transfer function in terms of wind speed and veer between the mast and reference dataset. Higher-order polynomials are also available;
b. *Matrix* [34]: a joint frequency distribution of the wind speed-up Δv and veer $\Delta\theta$ between the mast and reference series is built by binning the raw data in the concurrent period in a matrix form. This is then fitted through polynomial surfaces and used to generate the long-term corrected data time series either as it is (bootstrapping) or via a bivariate Gaussian distribution;
c. *Neural network* [35]*:* a machine learning algorithm is applied within the concurrent period of measured wind data and is used to train a neural network. The latter detects a pattern between the reference

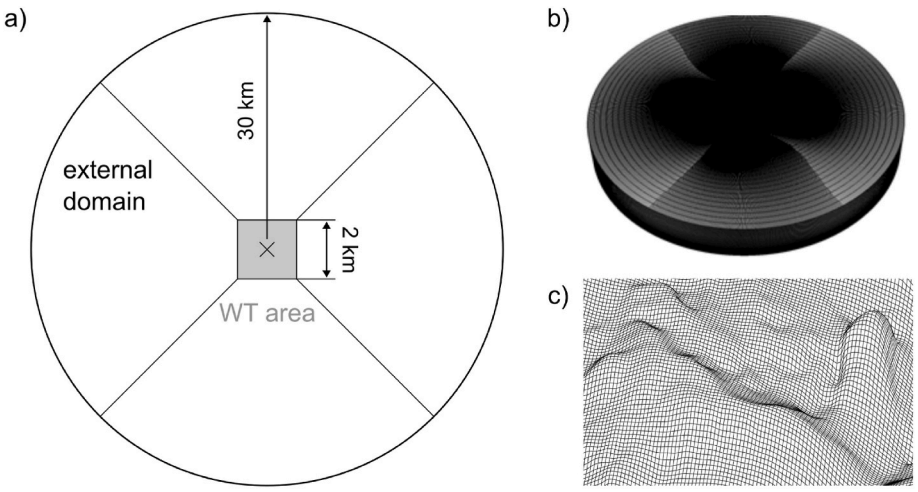

Fig. 5. Overview of the grid used for the site of Rivoli: a) computational domain b) external mesh c) wind turbines refinement region.

and the measured wind conditions and employs it to build the transfer function between the two.

In this study, all these methodologies were adopted and compared in terms of Mean Bias Error (MBE), Root Mean Square Error (RMSE) and correlation index *r*. The formulation giving the best values for these indexes was finally selected for the long-term correction.

3.2. WAsP

The WAsP linear extrapolation methodology [10] was used to compute the wind speed spatial distribution for each installation site based on the corresponding topology and anemometric measurements.

The core of this approach is presented by a spectral potential flow solver of the same family of MS3DJH methods [36], coupled with a simplified wall model that accounts for the effect of friction near the surface. This model is used to resolve the perturbations in the synoptic wind associated to the site orography, which is discretized via an ad-hoc polar grid. As highlighted by Wood et al. [37], this strategy tends to overestimate the speed-up associated with the presence of hills or ridges when their slope exceeds 20–30%, representing the major source of uncertainty in the analysis of complex terrains [10]. Mortensen et al. [26] tried to overcome this limitation by introducing an empirical correction based on the Ruggedness Index (RIX), but its use is extremely site-specific and generally not recommended in absence of sufficient data. For these reasons, this method was not considered herein.

The vertical profile *V(z)* of the Atmospheric Boundary Layer (ABL), on the other hand, is evaluated using a logarithmic law [17], as in Eq. (2):

$$V(z) = \frac{u_*}{k}\left[\ln\left(\frac{z}{z_0}\right) - \psi\left(\frac{z}{L}\right)\right] \tag{2}$$

where u^* is the friction velocity, which comes from the computation of the geostrophic drag, k is the Von Kármán constant, usually taken equal to 0.4, and z_0 is the effective roughness length. This is extracted from the input terrain roughness data via ad hoc interpolation. The second term in Eq. (2) accounts instead for buoyancy effects (atmospheric stability), using an empirical function ψ of the Monin-Obukhov length L (Eq. (3)):

$$L = \frac{T_0}{kg}\cdot\frac{C_P u_*^3}{H_0} \tag{3}$$

which depends on the surface temperature T_0 and heat flux H_0. The heat flux represents a setting parameter in WasP and must be tuned according to the specific stability conditions of each site, especially if heights higher than 50 m are of interest. According to Ref. [10], in fact stability effects are particularly relevant at high altitudes and low wind speeds. In the study, the default average heat flux value of -40 Wm^{-2} was adopted for all analyses. Although this choice introduces a non-negligible error in the estimation of the wind vertical profile and farm AEP, it allows for a more rigorous comparison between the considered sites by minimizing possible differences related to the WAsP set-up. On top of that, this gives the opportunity to highlight the weight of thermal modelling on the accuracy of this family of tools.

A dedicated model for the wake analysis of obstacles is also present in the WAsP formulation, which makes use of the Pereira semi-empirical correlation [38]. Its application is therefore limited to semi-infinite obstacles that are sufficiently far from critical calculation points, such as measurement masts or turbines.

3.3. WAsP-CFD

In WAsP-CFD, the potential flow approach embedded in WAsP is replaced by the three-dimensional Reynolds-Averaged Navier Stokes (RANS) EllypSys3D solver [39], developed at the Denmark Technical University (DTU).

The third-order QUICK upwind scheme is used for the discretization of convective terms and the Rhie-Chow interpolation for the pressure-velocity coupling. For turbulence closure, the approach adopts the standard k-ε model. In order to make simulations Reynolds-independent, the effects of the Coriolis force and atmospheric stability are neglected. This limits the relevant input variables to the wind inflow direction only and thus reduces the number of simulations to be carried out; on the other hand, the reliability of this approach on specific test sites is also limited, because the modelling of discussed effects still relies on WAsP (see Eq. (2)).

The site terrain is divided into squares of 2 × 2 km, and each of them is automatically discretized with a multi-block, structured mesh, as shown in Fig. 5b. The terrain surface is discretized with a cell size of 20 m, while 96 elements are used for the ABL along the vertical direction, progressively refining up to 5 cm in the near-surface region.

3.4. PARK

The PARK module is used to compute the AEP of the park from the combination of the wind speed profile at each WT hub height with the power curve of each turbine, which is provided as tabulated input. The so-called “stationary” approach available in windPRO was adopted, computing the AEP from the general wind statistics of the site without including time-varying phenomena such as the variation of the wind

Table 4
Losses considered for the estimation of the AEP in the sites under consideration.

Category	Type	Contribution	Range [%]
Wake interference	calculated	Wake losses, future wake effects	0.1–15
Availability	estimated	WT availability, grid availability, etc. …	3–4
Turbine performance	estimated/ calculated	Power curve, high wind hysteresis, wind flow, etc. …	1–2
Electric grid	estimated	Electrical losses, facility consumption, etc. …	2–4
Environment	estimated	Performance degradation due/not due to icing, shutdown due to icing, hail, lighting, etc. …	0.3–2
Curtailment	estimated	Wind Sector Management, noise, shadow flickering, birds, and chiropters, etc. …	NA
Other	estimated	–	1

freestream density with air temperature. For both extrapolation tools used herein, i.e., WAsP and WAsP-CFD, 12 wind sectors were considered for the computation, together with their associated Weibull distributions.

As recommended by Shakoor et al. [40], wake interference effects and the corresponding losses (see Table 4) were estimated with the N.O. Jensen Park 2 model [41], which assumes a linear expansion of the wake behind the turbine in the form of Eq. (4):

$$v(x) = V\left[1 - C_T\left(\frac{R}{R + \alpha \cdot x}\right)^2\right] \tag{4}$$

where v(x) is the velocity downstream of the turbine, V is the freestream wind speed, R is the rotor radius and C_T is the turbine thrust coefficient, taken from the corresponding curve. The constant α is the Wake Decay Constant (WDC), which was estimated for each sector by scaling the TI acquired at the mast, computed as the ratio between the standard deviation and the average of the measured wind data, for a default factor of 0.48.

The air density for each site, on the other hand, was estimated as the annual average of the on-site data coming from the mast and used to scale the available WT power curves accordingly. These are in fact commonly available for the default value of $\rho = 1.225$ kg/m^3.

3.5. Losses & Uncertainties (L & U)

The production analysis was eventually completed by computing for each site all the losses related to the annual operation of the park, in order to obtain the AEP available on the electric grid. This information was sided by the corresponding uncertainty, which is necessary in the phase of accessing funding for the wind farm project.

3.5.1. Losses

The average value of the AEP was derived from the one provided by the PARK calculation, i.e., AEP_{gross}, by subtracting the different losses contributions P_i:

$$AEP = AEP_{gross} \cdot \left(1 - \sum_i P_i\right) \tag{5}$$

Seven loss categories were identified, as reported in Table 4. Please refer to the windPRO user manual [42] for a more detailed explanation of each contribution. The corresponding values were assigned to each site based on either an automatic routine available in the software (*calculated*) or a combination of guidelines commonly adopted in the literature and indications from the installing company AGSM-AIM SpA (*estimated*).

Losses related to icing were considered only for the sites at an altitude above sea level higher than 500 m, i.e., *Casoni*, *Carpinaccio* and *Riparbella* (see Table 2), and estimated based on the corresponding IEA ice class from the WIceAtlas database [43]. No curtailment was included in the analysis.

3.5.2. Uncertainties

Along with the average energy production described in previous sections, the proper uncertainty interval was evaluated for each installation site. To highlight the role played by the quality of input wind data and terrain modelling choices on such estimation, individual uncertainty contributions were separated into two main classes: *model-* and *site-specific*. Uncertainties belonging to the first class change with the modelling strategy selected for the site and can be divided into four components:

- *MCP:* the uncertainty associated with the correlation between measured data and the reference one, necessary for the long-term effects correction (MCP). This uncertainty is here computed via the Klintø formulation [44]:

$$I = \sqrt{[1.55(1 - WI)]^2 + (0.06r^{-1.3})^2 + (0.2V)^2} \cdot Y^{-0.3} \cdot CF \tag{6}$$

where WI is the wind index for the concurrent period, r is the correlation coefficient, V is the wind speed variability in the reference series, Y is the number of concurrent years and CF is the conversion factor in terms of uncertainty between wind speed and AEP;

- *Interannual variability:* it represents the contribution associated with the year-to-year variability of the average wind speed in the 20-year reference dataset. It is simply evaluated by normalizing the corresponding standard deviation over $\sqrt{20}$;
- *Vertical extrapolation:* it is the uncertainty contribution connected to the difference in height between the measurement mast and the wind turbine hubs. It is computed as the linear combination of the difference in elevation above the sea level and the difference in height above the ground level between the two. A slope of 1%/10 m was adopted in the study, as recommended by the windPRO user manual for complex terrains [42];
- *Horizontal extrapolation*: it represents the uncertainty related to the different positions of the mast and the turbine hubs. It is computed in the same way as the contribution related to vertical extrapolation, using a sensitivity factor of 1.5%/km due to the complexity of terrains considered.

Site-specific uncertainties, on the other hand, are related to the general aspects of the wind farm operation and are mostly based on the user's experience or information made available by the installer. For example, one subgroup refers to the uncertainty related to the power curve of the installed WTs or to the metering of produced electric energy, while another is connected to the estimation of the losses. For the sake of brevity, recommended values for these parameters are not reported here but can be found in Ref. [42]. Among the different entries in this category, the uncertainty associated with the measurement of wind data is particularly important. A constant value of 3% was here selected for all sites, due to the overall good quality of the anemometric campaigns.

It must be noted that, in the case of uncertainty contributions evaluated directly from wind data, a scaling factor is needed to obtain the corresponding uncertainty on the AEP. In this case, this factor is automatically computed in the PARK module according to the region of the power curve in which the wind turbines are operating. Maximum sensitivity is expected in the linear part of the curve, decreasing towards the rated wind speed. In general, values between 1.6 and 2.4 are to be expected.

Table 5
Wind data used for the production analysis in the horizontal approach.

Name	Mast ID	Year	Height [m]	Ref. dataset	MCP method
Rivoli	1	2008–2009	50	EMD-WRF	Local scaling
Affi	1	2004–2005	50	EMD-WRF	Local scaling
Casoni di Romagna	2	2005–2006	30	EMD-WRF	Matrix
Carpinaccio	1	2006–2007	40	EMD-WRF	Matrix
Riparbella	1	2003–2004	30	EMD-WRF	Matrix

4. Results

In this section, the main results of the analysis are presented and critically analyzed. The first sub-section presents the results of the *horizontal approach*, highlighting the effects of the site terrain on the estimation of the corresponding AEP. Then, the impact of the modeling approach (spatial extrapolation using either WAsP or WAsP-CFD) and input data quality are further investigated in the sub-section regarding the *vertical approach*, applied specifically to the Rivoli site. In particular, the final scope of this analysis is to highlight the relationship between the complexity of the installation terrain and the fidelity required by the selected simulation tool.

4.1. "Horizontal" analysis approach

As discussed, in the *horizontal approach* the same workflow has been applied to all installation sites. This corresponds to the workflow commonly adopted in the industry and accepted so far by financing institutions for most of the installations. As noted in Section 3, only wind data at the most representative height and position for the site were considered for the analysis, as to mimic the very common case of an anemometric campaign based on a single-mast. Correction for wind interannual variability (MCP), on the other hand, was applied using data from the EMD-WRF dataset with the highest correlation, selecting the method with the minimum error. An overview of the adopted wind measurements for the different sites is reported in Table 5.

Fig. 6 shows the comparison between the predicted and measured AEP for all sites, with the corresponding uncertainty band. Results are normalized by the predicted P_{50} value. To support the discussion, the main contributions to the model-specific uncertainty, (i.e., the one dependent on input wind data and modelling choices) are also reported.

The sites for which the standard approach yields the best results are *Casoni* and *Carpinaccio*, with a relative error on the average AEP of approximately 3.5% and 8% respectively. The reason for such accuracy is twofold. On the one hand, these two cases are well characterized from an anemometric point of view, as the measurement mast experiences local flow conditions very similar to the actual ones on the turbines. This is apparent from Fig. 8, where the average wind speed maps obtained with the WAsP approach are reported for all sites. On top of that, the wind data used for the analysis are available at the same height of the WT hubs, thus minimizing the uncertainty associated with the vertical extrapolation of the wind profile (see Fig. 10). The same can be said for the database adopted for the long-term correction (EMD-WRF), as apparent from Fig. 8, resulting in the highest correlation in terms of wind speed with experimental measurements among all sites (see Fig. 7). In the case of *Casoni* nonetheless, due to the inability of the WRF mesoscale simulation to resolve the ridge where the mast is installed (see Fig. 9), the uncertainty associated with the MCP procedure has a higher

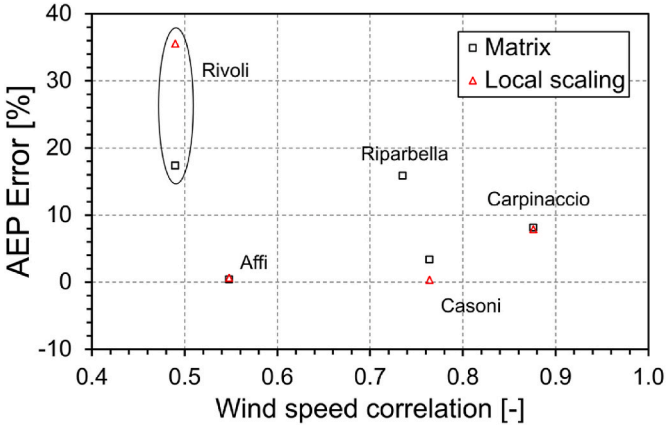

Fig. 7. Trend of the error on the predicted AEP with respect to the quality of correlation between short- and long-term data, for different correlation methodologies and installation sites.

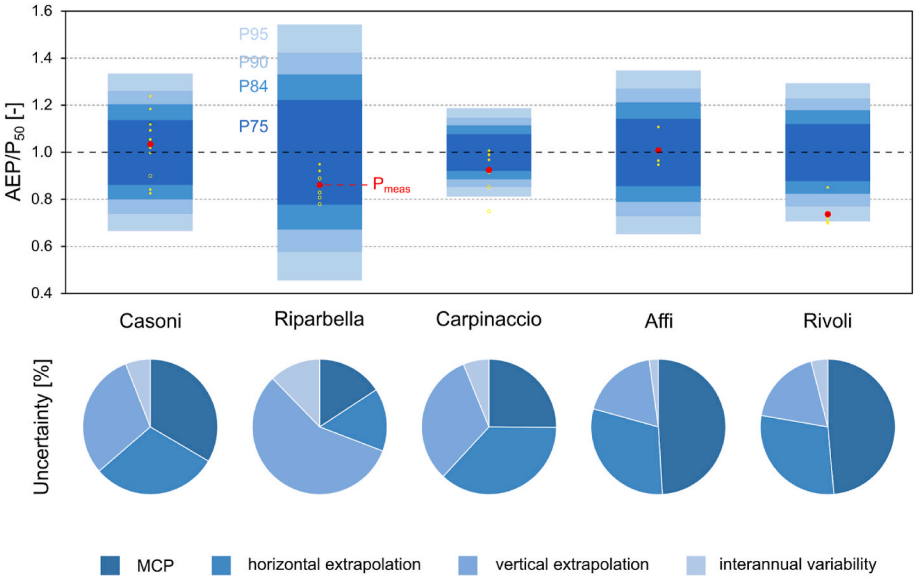

Fig. 6. Comparison in terms of measured and predicted AEP, with the corresponding uncertainty, for all installation sites. Individual contributions to model-specific uncertainty are also reported.

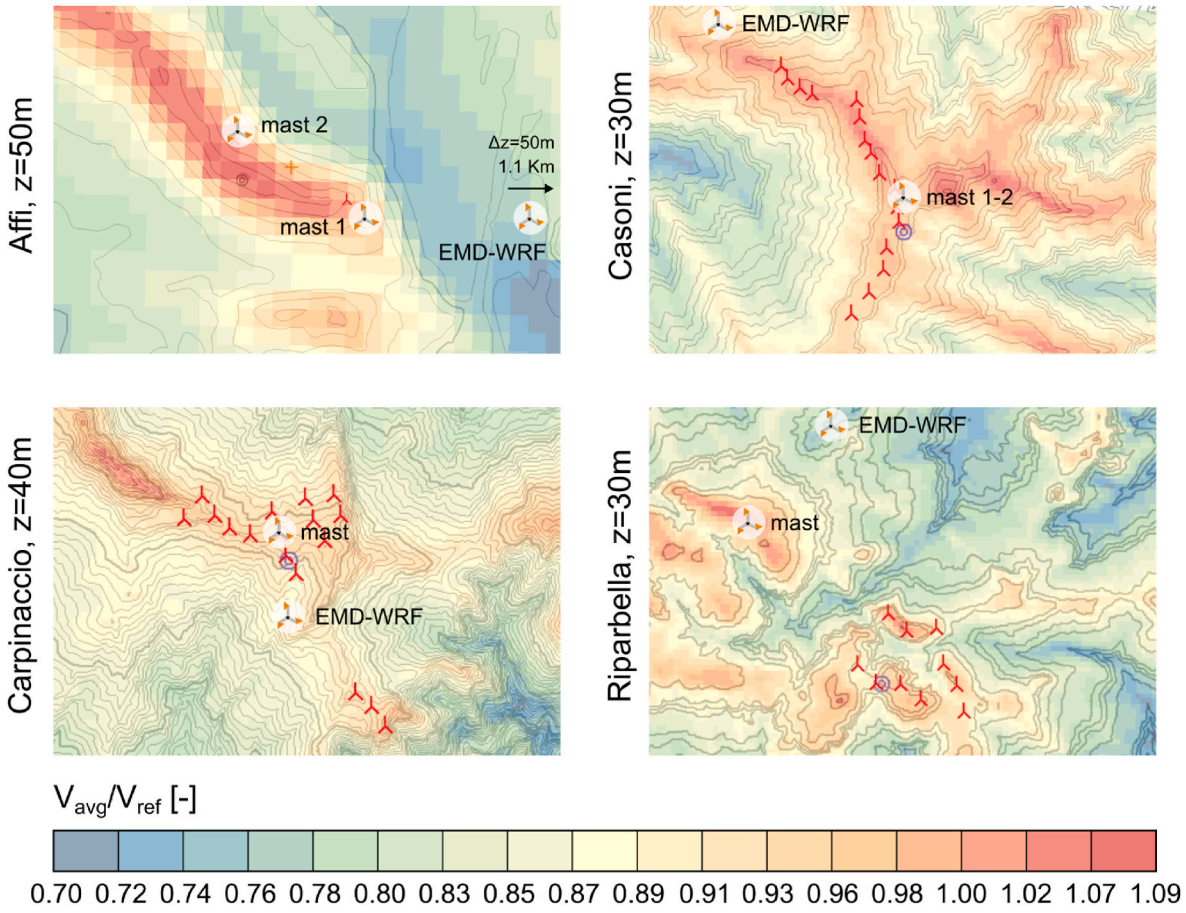

Fig. 8. Comparison in terms of average wind speed map for the sites under consideration.

impact. The situation is made worse by the location of the EMD-WRF grid node at the edge of the ridge, where it might experience some deviation in the synoptic flow due to the presence of the ridge itself. On the other hand, these two sites present characteristics that are compatible with the WAsP linear approach, according to the limitations outlined in Section 3.2. Wind speed oscillations due to diurnal thermal forcing are in both cases mild (see Fig. 3), resulting, especially for the site of *Casoni*, in a good fitting of the experimental wind speed profile with the logarithmic law, as shown by Fig. 10. This trend is also justified by a relatively simple altimetric profile of the ridge where both the WTs and the mast are installed along the main wind direction (SSW). The ridge is steeper for *Carpinaccio*, with a slope of approximately 40%, thus exceeding the 30% value normally set as a threshold for the WAsP approach [25]. This might explain the higher discrepancy of the predicted AEP with respect to the measured one, as flow separation on the leeward side of the ridge might occur in real operating conditions, shadowing some of the turbines (see Fig. 6).

The same degree of accuracy in terms of AEP can be observed for *Affi,* with an error of 0.6%, as in Fig. 6. However, this result needs a more careful examination as it might come from the compensation of different error sources. In fact, although the measurement mast is in the same flow area as the WTs (see Fig. 8), the maximum measurement height available is only 60% of the hub height. Combined with the low quality of the dataset used for the long-term correction, which is located 1.1 km away from the site center and 50 m higher (see Fig. 8), this configuration results in a high uncertainty on the computed AEP, mainly due to the MCP contribution (see Fig. 6).

Another interesting feature of this installation site is that, despite its strong diurnal thermal excursion (see Fig. 3), the boundary layer predicted by WAsP (default set-up, see Section 3.2) is quite stable in correspondence of mast #1.This is apparent in Fig. 10, and the boundary layer prediction seems to be adequate for the estimation of the farm's AEP. This can be simply related to the simpler orography of *Affi* with respect to other sites, although a role could also be played by a balancing effect between the energy produced during the first and second halves of the day, with a relatively low seasonal variation.

If the analysis of the sites considered so far yields overall reasonable results in terms of estimated energy production, for the last two, i.e., *Riparbella* and *Rivoli*, the accuracy of the approach is considerably lower, with *Riparbella* presenting a relative error on the AEP of about 14% and by far the highest uncertainty. The reason for this can be found in the fact that in such a complex terrain (see Fig. 2), where the anemometric campaign should be performed as close as possible to the site center, the measurement mast was instead located on a different ridge, as shown in Fig. 8. As a matter of fact, based on its altimetric profile (see Fig. 10), the mast location could have been subject to flow separation, with a consequent underestimation of the measured wind speed with respect to the one experienced by the farm. This effect cannot even be taken into account by WAsP, as it lies outside of its range of validity. As the maximum measurement height is also less than half of the WT hubs' one, the combination of uncertainties related to vertical and horizontal extrapolations contribute to 70% of the total uncertainty in AEP. The contribution of the MCP correction is not negligible either, since the WRF simulation completely bypasses the local terrain configuration, as in the case of *Casoni*. Upon combination of Figs. 8 and 9, it can be seen in particular how the grid of the reference model is not able to resolve the small low-speed valley where the EMD-WRF node is positioned.

Finally, special attention is deserved by the site of *Rivoli*, which was shown to be the most complex installation site. As expected, this complexity made it the case for which the standard approach based on

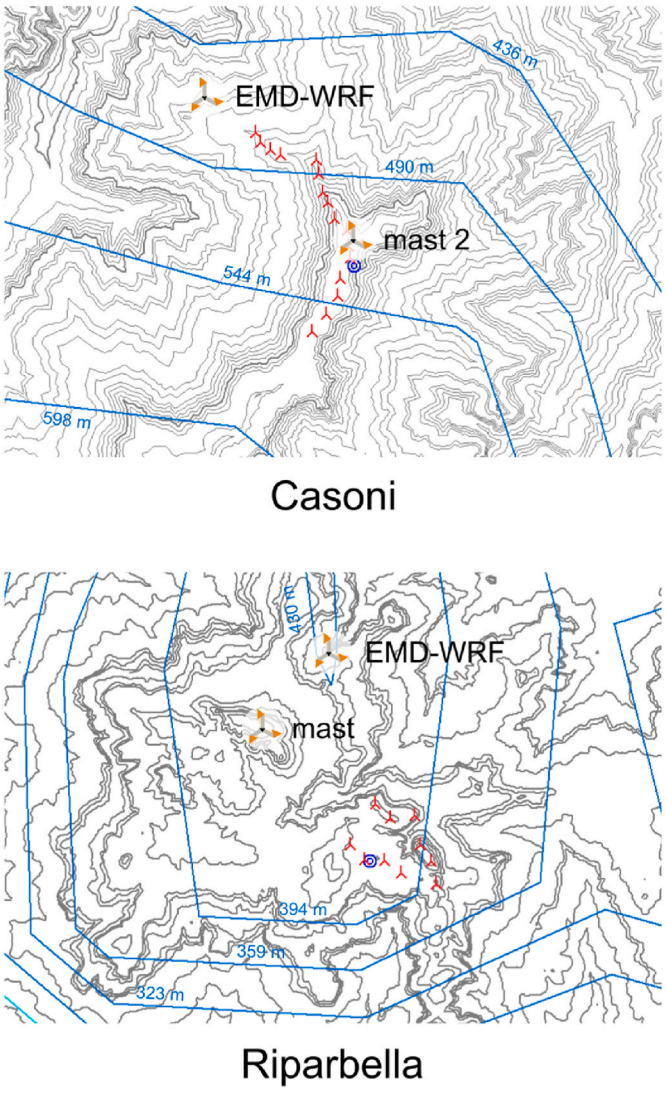

Fig. 9. Comparison in terms of terrain resolution between the orography map at the micro-scale (grey) and the one available in the mesoscale model EMD-WRF (blue) for the sites of *Casoni* and *Riparbella*.

WAsP presents the worst accuracy, with an error on AEP of approximately 28% lying at the edge of the uncertainty interval. The reason for this very high uncertainty value is not connected to measured wind data themselves, as the mast selected for the analysis (mast #1) is representative of the wind conditions on the ridge (see Fig. 14) and has a 7-year acquisition period (the longest among all sites under consideration - see Table 3). A major contribution to the overall uncertainty is instead introduced by the peculiar characteristics of the site, which present a strong diurnal heat forcing (see Fig. 3) and a complex orography with a slope along the main wind direction exceeding 40%. As described in the following Section 4.2, one of the peculiarities of this park is that the ridge where the WTs are installed is very different from the semi-infinite hills on which the calibration and verification of linear models are usually based [36]; this is particularly evident for the east side, where the ridge abruptly goes down to the valley of the river Adige (see Fig. 2). Therefore, the WAsP approach is expected to fail in predicting the flow development in that area. The MCP correction is also relevant since, as shown in Fig. 6, it accounts for almost half of the model-specific uncertainty due to the very low correlation of the reference data with measured ones. The reason for this trend is explained in detail in Section 4.2. It must be noted how, as reported in Fig. 7, in these specific conditions the AEP estimation is extremely sensitive to the adopted MCP methodology, especially when choosing between a *Local Scaling* approach and one like *Matrix* that also modifies the predicted wind direction.

4.2. "Vertical" analysis approach - Rivoli

In the vertical approach, the site of *Rivoli* was selected as a test case for comparing different strategies for the pre-processing of on-site anemometric measurements as well as spatial extrapolation models. The baseline case for all the analyses presented in the following sections is the set-up used for the horizontal approach, as reported in Table 5.

Upon examination of Fig. 11, Fig. 12, and Fig. 13, it can be observed how the introduction of the WAsP-CFD extrapolation immediately increased the accuracy of the predicted farm AEP for all considered cases, with a deviation with respect to measured data 15% lower than the one achieved with WAsP. Such improvement is related to the better resolution of the interaction between the synoptic wind and the site's complex orography, for which the standard WAsP formulation is barely valid (see Section 3.2). Nevertheless, the CFD-based approach still overestimates by approximately 23% the real production of the farm. Among the many possible explanations, one of the most reasonable is that neither WAsP nor WAsP-CFD can take into account the strong diurnal heat forcing effects affecting the site (see Fig. 3), for which, in contrast with *Affi* (see Section 4.1), a net positive outcome on the computed AEP is seen. Such a deviation could be partially compensated by tuning the heat flux parameters available in the WAsP model (see Eq. (3)). This is, however, out of the scope of the present study, in view of ensuring modeling uniformity in the comparative analysis.

4.2.1. Effect of input wind data

Fig. 11 aims to identify a trend between the error obtained in the prediction of the AEP and the correlation in terms of wind speed between the measured short-term data and the long-term reference ones. Various combinations of the two datasets, such as different years of measurement and reanalysis databases, are investigated. As already observed for the other sites under consideration (see Fig. 7), the AEP error tends to decrease with the quality of the correlation. For instance, a 10% lower correlation corresponds to a 10% higher error on the estimated energy production. For very low correlation indexes, as in the case of the ERA5T data series, deviation with respect to measured data becomes unacceptable and the corresponding uncertainty reaches unphysical values. Therefore, it is not reported on the graph. It is interesting to note that this trend is conserved when switching from WAsP to WAsP-CFD, implying the mutual independence between the MCP analysis and the adopted extrapolation model.

When focusing on the impact of different measurement heights on the generation of the wind statistics, it is clearly visible from Fig. 12 how, for the WAsP approach, the error in the AEP steadily decreases as the instrumentation gets closer to the WT hub heights, in terms of both average value (−20%) and standard deviation. Due to the presence of the Atmospheric Boundary Layer (ABL), the reduction rate is however not constant, but increases once a certain threshold height is exceeded. From a practical point of view, this means that, if measurements at multiple heights are not possible, the selection of the sensors' height deserves special attention and likely additional costs due to a taller mast could be easily paid back by a much better final estimation of AEP. WAsP-CFD is instead way less sensitive than WAsP to the measurement height, with a maximum oscillation of ±5% for the present case. This is related to the higher modelling capabilities offered by this tool for complex terrains. It is also worth noticing that, differently from WAsP, the uncertainty associated with the AEP estimation seems to be constant with the selected height.

Finally, the effect of the position of the measurement mast was investigated. As apparent from Fig. 13, although masts #1 and #2 lie at the two extremes of the ridge where the turbines are installed (see Fig. 14) and the distance between them is only 900 m, picking one or

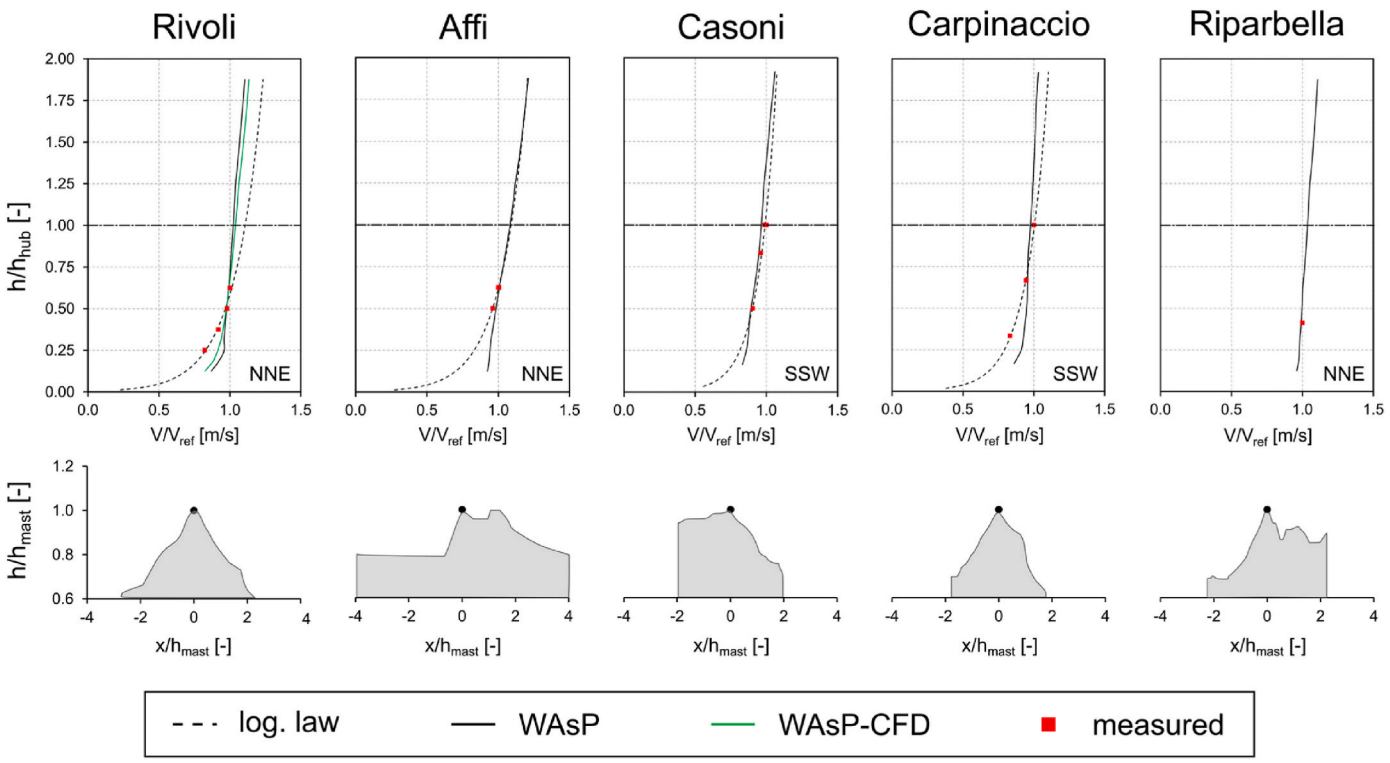

Fig. 10. Comparison in terms of average wind speed vertical profile between measured data and the adopted extrapolation models.

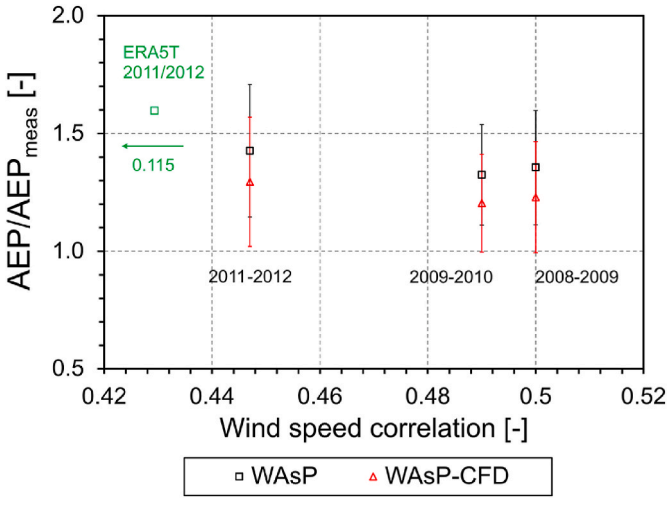

Fig. 11. Trend of the error on the predicted AEP with respect to the quality of correlation between short- and long-term data for the site of *Rivoli*. Different measurement years and reference datasets are considered for mast #1, z = 50 m. MCP correction is performed with the Local Scaling method.

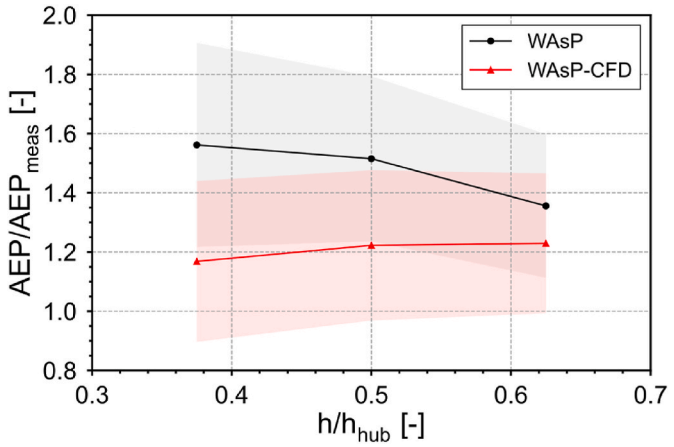

Fig. 12. Trend of the error on the predicted AEP with respect to the measurement height selected for the PARK computation for the site of *Rivoli*.

another leads to largely over- or underestimating the park energy production, respectively. This holds for both WAsP and WAsP-CFD, although for the latter the sensitivity to input wind data is once again lower. Such behavior is strictly connected to the difference in flow conditions experienced by the two measuring towers, as visible in Fig. 14 and thoroughly described in the next paragraph.

4.2.2. Effect of extrapolation model

To gain a better understanding of how the site terrain affects the corresponding wind distribution and how this is related to the accuracy of the extrapolation method, in this section the flow fields obtained with the WAsP and WAsP-CFD formulations are reported and compared. The reference set-up is the same as that used for the *horizontal approach*, which here represents the baseline.

Fig. 14 shows the map of the speed-up factor, i.e., the ratio between the local wind speed and the undisturbed one, obtained with WAsP-CFD in the main wind direction of the site (NNE) at the WT hub (z = 80 m). As highlighted in Section 3.3, the use of this variable is made possible by the Reynolds-independent formulation of WAsP-CFD. The vertical development of the flow in correspondence of the two masts is also reported (traverses T1 and T2). It can be observed in general how the ridge where the WTs are installed is interested by a fairly uniform acceleration of the flow (up to +20%) along its span. As visible from traverse T1, this flow pattern is at the very limit of the modelling domain of linear methods like WAsP, with a small recirculation region already developing downstream the ridge peak. Thanks to its location, mast #1 is

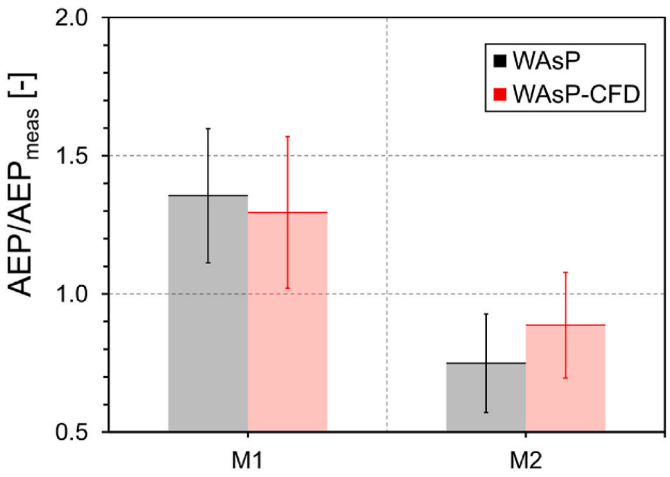

Fig. 13. Error on the predicted AEP with respect to the mast selected for the analysis, considering the reference year 2011/2012 and z = 50 m.

representative of this behavior. Approaching its edges, the ridge flow is progressively disrupted. On the eastern side where the last turbine and mast #2 are installed, the wind is characterized by a lower speed and veers towards the northern direction, due to the combined influence of edge effects [6] and the development of a massive recirculation region in the adjacent valley downstream. The latter is provoked by the steep pressure gradient associated with the cliff leading from the edge of the ridge to the basin of the river Adige. These features are also clearly visible in the anemometric measurements of mast #2 reported in Fig. 3 and they are responsible for the underprediction observed when using this data to compute the park annual energy production (see Fig. 13).

The flow pattern described so far is inherently challenging for linear tools such as WasP, whose accuracy degrades rapidly for steep and low-aspect-ratio ridges like the one under consideration [26]. In order to quantify this limitation, Fig. 15 reports a contour plot of the ratio between the wind speed velocities, averaged over the year and the considered wind sectors, predicted by WAsP and WAsP-CFD, respectively, for the baseline set-up at the maximum measurement height of z = 50 m. This metric allows one to highlight where most of the discrepancies between the methods are located. From a perusal of Fig. 15, it is apparent that WAsP tends to overpredict the acceleration of the flow over the whole ridge, up to a maximum of approximately +50% with respect to the CFD approach. In correspondence of mast #2, this error rises to +60%, as the effects of downstream separation are completely absent. In that region, WAsP estimates a wind speed that is more than double than that of WAsP-CFD. Based on these observations, it is possible to understand why, for this specific installation site, the standard approach always tends to predict an AEP higher than the CFD and the measured ones (confirmed by Figs. 11, Figure 12, and Fig. 13).

4.2.3. *Effect of reference data*

The complex terrain of *Rivoli* affects not only the performance of the extrapolation model (WAsP or WAsP-CFD) used for the analysis, but also the maximum accuracy attainable from the MCP correction. It has already been observed in Section 4.1 that this site has in fact the lowest correlation between the mast and reference data (see Fig. 7) and, as a consequence, one of the highest levels of uncertainty related to the long-term correction, as shown in Fig. 6.

This specific problem lies, as highlighted in Fig. 16, in the mismatch between the level of detail required to resolve the ridge where the turbines are installed and the one provided by the WRF simulation, which has a maximum resolution of 3 km (which is anyhow a quite refined one among the databases commonly in use for industrial applications). As a matter of fact, the WRF model here completely bypasses the ridge, predicting a local wind time history that is not characterized by the same speed-up effect as the local measurements. A relevant error is thus introduced in the computation of the farm AEP for all the adopted correlation methodologies. It is worth remarking that in installation sites like *Rivoli* this happens despite the WRF grid node being very close to the reference mast, as shown in Fig. 16.

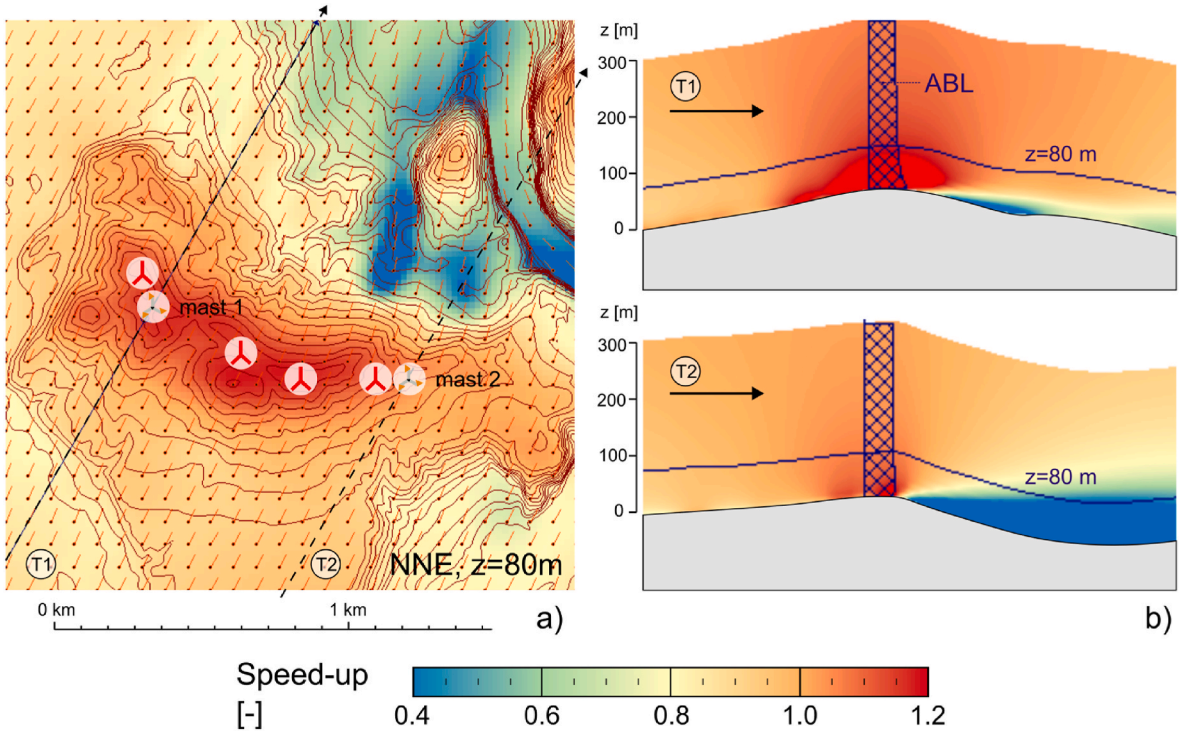

Fig. 14. Speed-up factor contour obtained with WAsP-CFD for the site of *Rivoli* along the main wind direction (NNE): a) horizontal plane at hub height, z = 80 m b) vertical plane along the traverses T1 and T2.

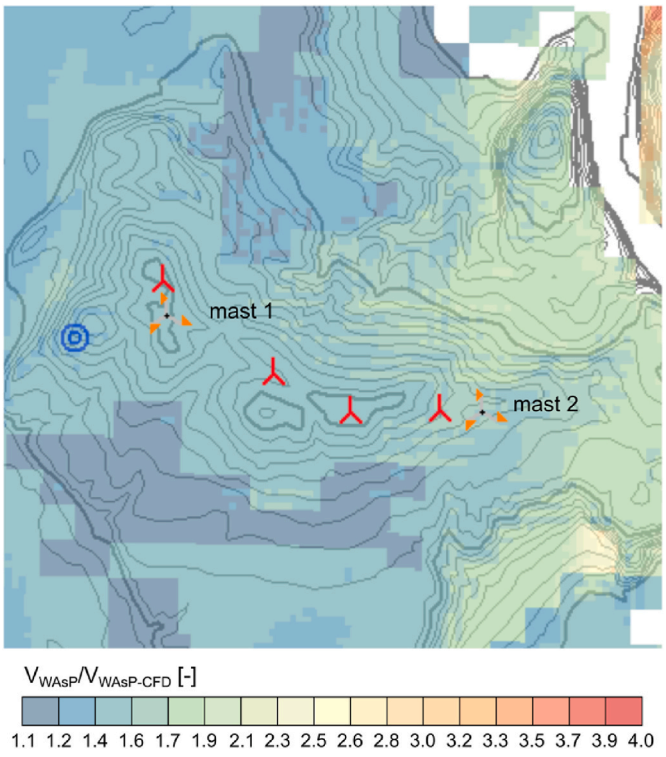

Fig. 15. Map of the error in terms of average wind speed between the WAsP and WAsP-CFD predictions for the site of *Rivoli*, at the maximum measurement height of z = 50 m.

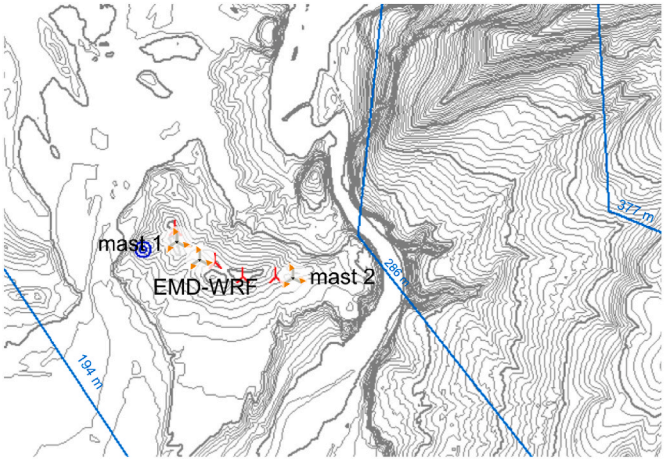

Fig. 16. Comparison in terms of terrain resolution between the local orography map (grey) and the one available to the mesoscale model EMD-WRF (blue) for the site of *Rivoli*.

5. Conclusions

In this study, the uncertainty associated with the on-field anemometric campaign and the extrapolation of these wind data over complex terrains on the predicted production of a wind farm was investigated. Five different sites in Italy, for which the installing company had *a posteriori* AEP data available, were considered for the analysis. Two different approaches were followed. In the "*horizontal*" one, the minimum amount of wind data common to all installation sites was used, i.e., the measurement of one mast at one selected altitude for one year, thus highlighting the role of the terrain modelling. In the "*vertical*" approach, the analysis focused on the site with the most complex terrain, using wind data of different quality and duration as well as different processing techniques, from the common WAsP linear formulation to the more advanced WAsP-CFD method. Based on the results of these analyses, the following conclusions can be drawn:

- The capability of measured wind data to represent the average flow conditions affecting the farm is key for any AEP calculation. In this perspective, it is not sufficient to place the mast as close as possible to the site center and the acquisition system as close as possible to the height above ground level of the turbine hubs; it must also be ensured that the mast location is not a critical one, i.e., affected by local flow separation or thermally induced secondary flows. The same requirements need to be imposed on the reference data series used for the long-term correction. In fact, for low levels of correlation between the short- and long-term datasets, the uncertainty associated with the long-term extrapolation can represent more than half of the total.
- The quality of input wind data becomes more and more important as the reliability of the adopted extrapolation model is reduced. For the site of *Rivoli*, for instance, a +60% increase in the measurement height is required to obtain an accuracy comparable with that of WAsP-CFD with a linear model such as WAsP. Conversely, if a high-fidelity extrapolation model is used, less effort can be put into gathering accurate on-site measurements.
- In very complex terrains, where orographic characteristics are far from the semi-infinite hill used for the construction of linear models, advanced extrapolation techniques such as WAsP-CFD are required even in presence of high-quality wind data from multiple measurement points. This confirms the trends highlighted in the scientific literature on the matter. As a matter of fact, the interaction of the wind with the local terrain can lead to flow conditions on each turbine that are substantially different from those experienced by the mast or by the other turbines. On top of that, linear models like WAsP tend to overestimate (up to +60% in the case of *Rivoli*) the speed-up effect of hills with a slope higher than 30%, especially when flow separation occurs downstream.
- The effects of thermal forcing are strongly site-specific, as their influence on the wind resource and the AEP depends on their time history over the year and their interaction with other phenomena affecting complex terrains. Therefore, adequate tuning of the adopted extrapolation model, such as WAsP, is pivotal. Presently, the common practice is to compare the WAsP vertical profile with one extrapolated from mast data using a time-based wind shear measured matrix. As this approach is not exempt from theoretical flaws, more research must be spent in that direction.

CRediT authorship contribution statement

P.F. Melani: Methodology, Software, Validation, Formal analysis, Investigation, Data curation, Writing – original draft, Visualization. **F. Di Pietro:** Methodology, Software. **M. Motta:** Methodology, Writing – review & editing, Supervision. **M. Giusti:** Resources, Supervision. **A. Bianchini:** Conceptualization, Methodology, Investigation, Resources, Data curation, Writing – review & editing, Supervision, Project administration, Funding acquisition.

Declaration of competing interest

The authors declare that they have no known competing financial interests or personal relationships that could have appeared to influence the work reported in this paper.

Data availability

The data that has been used is confidential.

Acknowledgements

The authors would like to acknowledge Dr. Francesco Papi from the Università degli Studi di Firenze for his help in the site analyses with windPRO, as well as Prof. Giovanni Ferrara of the same institution for its support of this research program. Thanks are also due to Dr. Alberto Venturi and Dr. Andrea Scala from AGSM AIM for providing experimental wind data and sites' features.

References

[1] Global Wind Report 2022. Global wind energy Council. 2022. https://gwec.net/global-wind-report-2022/. [Accessed 4 May 2022]. accessed.
[2] Murthy KSR, Rahi OP. A comprehensive review of wind resource assessment. Renew Sustain Energy Rev 2017;72:1320–42. https://doi.org/10.1016/j.rser.2016.10.038.
[3] Friis Pedersen T, Gjerding S, Ingham P, Enevoldsen P, Kjaer Hansen J, Kanstrup Joergensen H. Wind turbine power performance verification in complex terrain and wind farms. 2002.
[4] Alfredsson PH, Segalini A. Introduction Wind farms in complex terrains: an introduction. Phil Trans Math Phys Eng Sci 2017;375:20160096. https://doi.org/10.1098/rsta.2016.0096.
[5] Barber S, Schubiger A, Koller S, Eggli D, Radi A, Rumpf A, et al. A new decision process for choosing the wind resource assessment workflow with the best compromise between accuracy and costs for a given project in complex terrain. Energies 2022;15:1110. https://doi.org/10.3390/en15031110.
[6] Fernando HJS, Mann J, Palma JMLM, Lundquist JK, Barthelmie RJ, Belo-Pereira M, et al. The Perdigão: peering into microscale details of mountain winds. Bull Am Meteorol Soc 2019;100:799–819. https://doi.org/10.1175/BAMS-D-17-0227.1.
[7] Clifton A, Daniels MH, Lehning M. Effect of winds in a mountain pass on turbine performance. Wind Energy 2014;17:1543–62. https://doi.org/10.1002/we.1650.
[8] Fernando HJS, Pardyjak ER, Sabatino SD, Chow FK, Wekker SFJD, Hoch SW, et al. The MATERHORN: unraveling the intricacies of mountain weather. Bull Am Meteorol Soc 2015. https://doi.org/10.1175/BAMS-D-13-00131.1. 96:1945–67.
[9] Whiteman CD, Doran JC. The relationship between overlying synoptic-scale flows and winds within a valley. J Appl Meteorol 1993;32:1669–82.
[10] Troen I, Lundtang Petersen E. European wind Atlas. Roskilde: Risø National Laboratory; 1989.
[11] Troen I, Hansen BO. Wind resource estimation in complex terrain: prediction skill of linear and nonlinear micro-scale models. 2015.
[12] Ayotte KW. Computational modelling for wind energy assessment. J Wind Eng Ind Aerod 2008;96:1571–90. https://doi.org/10.1016/j.jweia.2008.02.002.
[13] Yan BW, Li QS. Coupled on-site measurement/CFD based approach for high-resolution wind resource assessment over complex terrains. Energy Convers Manag 2016;117:351–66. https://doi.org/10.1016/j.enconman.2016.02.076.
[14] Tabas D, Fang J, Porté-Agel F. Wind energy prediction in highly complex terrain by computational fluid dynamics. Energies 2019;12:1311. https://doi.org/10.3390/en12071311.
[15] Banta RM, Pichugina YL, Kelley ND, Hardesty RM, Brewer WA. Wind energy meteorology: insight into wind properties in the turbine-rotor layer of the atmosphere from high-resolution Doppler lidar. Bull Am Meteorol Soc 2013;94:883–902. https://doi.org/10.1175/BAMS-D-11-00057.1.
[16] Raupach MR. Simplified expressions for vegetation roughness length and zero-plane displacement as functions of canopy height and area index. Boundary-Layer Meteorol 1994;71:211–6. https://doi.org/10.1007/BF00709229.
[17] Gualtieri G. A comprehensive review on wind resource extrapolation models applied in wind energy. Renew Sustain Energy Rev 2019;102:215–33. https://doi.org/10.1016/j.rser.2018.12.015.
[18] Lopes da Costa JC, Castro FA, Palma JMLM, Stuart P. Computer simulation of atmospheric flows over real forests for wind energy resource evaluation. J Wind Eng Ind Aerod 2006;94:603–20. https://doi.org/10.1016/j.jweia.2006.02.002.
[19] Venkatraman K, Hågbo T-O, Buckingham S, Teigen Giljarhus KE. Effect of different source terms and inflow direction in atmospheric boundary modeling over the complex terrain site of Perdigão. Wind Energy Science 2023;8:85–108. https://doi.org/10.5194/wes-8-85-2023.
[20] Pérez Albornoz C, Escalante Soberanis MA, Ramírez Rivera V, Rivero M. Review of atmospheric stability estimations for wind power applications. Renew Sustain Energy Rev 2022;163:112505. https://doi.org/10.1016/j.rser.2022.112505.
[21] Letzgus P, Guma G, Lutz T. Computational fluid dynamics studies on wind turbine interactions with the turbulent local flow field influenced by complex topography and thermal stratification. Wind Energy Science 2022;7:1551–73. https://doi.org/10.5194/wes-7-1551-2022.
[22] Lei M, Shiyan L, Chuanwen J, Hongling L, Yan Z. A review on the forecasting of wind speed and generated power. Renew Sustain Energy Rev 2009;13:915–20. https://doi.org/10.1016/j.rser.2008.02.002.
[23] Chandel SS, Ramasamy P, Murthy KSR. Wind power potential assessment of 12 locations in western Himalayan region of India. Renew Sustain Energy Rev 2014;39:530–45. https://doi.org/10.1016/j.rser.2014.07.050.
[24] Kucukali S, Dinçkal Ç. Wind energy resource assessment of izmit in the west black sea coastal region of Turkey. Renew Sustain Energy Rev 2014;30:790–5. https://doi.org/10.1016/j.rser.2013.11.018.
[25] Rathmann O, Mortensen NG, Landberg L, Bowen A. Assessing the accuracy of WAsP in non-simple terrain. Wind Energy Conv. 1996:413–8. 1996 Proceedings.
[26] Mortensen NG, Bowen AJ, Antoniou I. Improving WAsP predictions in (too) complex terrain: 2006 European wind energy conference and exhibition. Proceedings (Online) 2006.
[27] Barber S, Schubiger A, Koller S, Eggli D, Radi A, Rumpf A, et al. The wide range of factors contributing to wind resource assessment accuracy in complex terrain. Wind Energy Science 2022;7:1503–25. https://doi.org/10.5194/wes-7-1503-2022.
[28] Tarquini S, Isola I, Favalli M, Battistini A. TINITALY, a digital elevation model of Italy with a 10 meters cell size. 2007. https://doi.org/10.13127/TINITALY/1.0.
[29] Büttner G, Kosztra B, Kleeschulte S, Hazeu G, Vittek M, Schröder C, et al. CORINE Land cover product user manual (version 1.0). Copernicus Land Monitoring Service; 2021.
[30] Thøgersen ML, Svenningsen L, Sørensen T, Jogararu M. EMD-WRF global on-demand mesoscale services: ERA5, ERA-interim, MERRA2 and CFSR. EMD International A/S; 2018.
[31] Joensen A, Landberg L, Madsen H. A new measure-correlate-predict approach for resource assessment. 1999.
[32] Hersbach H, Bell B, Berrisford P, Hirahara S, Horányi A, Muñoz-Sabater J, et al. The ERA5 global reanalysis. Q J R Meteorol Soc 2020;146:1999–2049. https://doi.org/10.1002/qj.3803.
[33] Mann HB. Nonparametric tests against trend. Econometrica 1945;13:245–59. https://doi.org/10.2307/1907187.
[34] Woods JC, Watson SJ. A new matrix method of predicting long-term wind roses with MCP. J Wind Eng Ind Aerod 1997;66:85–94. https://doi.org/10.1016/S0167-6105(97)00009-3.
[35] Addison JFD, Hunter A, Bass JH, Rebbeck M. A neural network version of the measure correlate predict algorithm for estimating wind energy yield. 2000.
[36] Jackson PS, Hunt JCR. Turbulent wind flow over a low hill. Q J R Meteorol Soc 1975;101:929–55. https://doi.org/10.1002/qj.49710143015.
[37] Wood N. The onset of separation in neutral, turbulent flow over hills. Boundary-Layer Meteorol 1995;76:137–64. https://doi.org/10.1007/BF00710894.
[38] Perera MDAES. Shelter behind two-dimensional solid and porous fences. J Wind Eng Ind Aerod 1981;8:93–104.
[39] Sørensen NN. General purpose flow solver applied to flow over hills. Doctoral thesis. Risø National Laboratory; 1995.
[40] Shakoor R, Hassan MY, Raheem A, Wu Y-K. Wake effect modeling: a review of wind farm layout optimization using Jensen's model. Renew Sustain Energy Rev 2016;58:1048–59. https://doi.org/10.1016/j.rser.2015.12.229.
[41] Katic I, Højstrup J, Jensen NO. A simple model for cluster efficiency: European wind energy association conference and exhibition. EWEC'86 Proc. 1987;1:407–10.
[42] WindPRO user manual 3.5: energy. EMD International A/S; 2021.
[43] Rissanen S, Lehtomäki V. Wind power icing Atlas (WIceAtlas) & icing map of the world. Piteå; 2015.
[44] Klintø F. Long-term correction - uncertainty model using different long-term data. 2015. London.